REPORT

PLANETARY TOPOGRAPHY

Global drainage patterns and the origins of topographic relief on Earth, Mars, and Titan

Benjamin A. Black,[1,2]* J. Taylor Perron,[3] Douglas Hemingway,[4] Elizabeth Bailey,[5] Francis Nimmo,[6] Howard Zebker[7]

Rivers have eroded the topography of Mars, Titan, and Earth, creating diverse landscapes. However, the dominant processes that generated topography on Titan (and to some extent on early Mars) are not well known. We analyzed drainage patterns on all three bodies and found that large drainages, which record interactions between deformation and erosional modification, conform much better to long-wavelength topography on Titan and Mars than on Earth. We use a numerical landscape evolution model to demonstrate that short-wavelength deformation causes drainage directions to diverge from long-wavelength topography, as observed on Earth. We attribute the observed differences to ancient long-wavelength topography on Mars, recent or ongoing generation of long-wavelength relief on Titan, and the creation of short-wavelength relief by plate tectonics on Earth.

Increasingly detailed observations of rocky and icy bodies in our solar system reveal dramatic diversity in surface topographic features. Plate tectonics has shaped topography extensively on Earth, but on less tectonically active worlds like Mars (*1*–*5*), and icy worlds like Titan and Pluto (*6*–*8*), the origins and history of the observed surface topography are varied and in some cases unknown. Fluid erosion offers a means to probe the long-term evolution of topography because drainage patterns interact with topography as it is uplifted and eroded [e.g., (*9*)]. Fluid runoff has shaped the surfaces of at least three bodies in the solar system in the form of liquid water on Earth and Mars [e.g., (*10*)] and liquid hydrocarbons on Titan [e.g., (*11*, *12*)], thereby inscribing a record of how the development of landscapes has differed on these three worlds.

Earth's topography is dominated by the dichotomy between continents and ocean basins; most rivers drain from continental interiors to the ocean. However, Earth's topography is also shaped by deformation concentrated near plate boundaries, such as the formation of collisional mountain ranges or volcanic arcs above subduction zones. These features can divert rivers as they traverse continents and can thereby displace drainage divides toward active margins, reshaping some of the planet's richest ecosystems in the process (*13*). Many terrestrial river basins in tectonically active regions are continuously reorganized in response to changing tectonic boundary conditions (*9*). As fluvial erosion (i.e., erosion by surface liquid flow) competes with tectonic deformation to shape Earth's landscapes, global drainage patterns should come to reflect a combination of long-wavelength, continent-scale topography and shorter-wavelength features such as mountain ranges.

Large-scale topography on Mars was established more than 3.5 billion years ago (Ga) in the wake of the formation of Borealis Basin (*4*, *14*) and the growth of the Tharsis volcanic rise (*1*). Most fluvial activity likely occurred early in the planet's history (*5*, *10*, *15*). On Titan, sparse impact craters and mountainous terrains attest to active modification of the surface (*16*), though the age and origin of relief and the tempo of erosional modification remain to be determined (*11*). We consider whether global drainage patterns differ on Earth and Mars as a result of their divergent geologic and surface histories, and we explore the implications of that comparison for Titan and other bodies where the erosional and tectonic history is largely unknown.

Our hypothesis is that on planets or moons where long-wavelength processes dominate production of relief, drainages should generally flow parallel to the slope of the long-wavelength topography, and the correlation should improve only marginally as the resolution of the topography is refined. We term the agreement between drainage patterns and topography at a given scale the "drainage conformity with topography." In this context, we consider topography to be long-wavelength if it spans at least 1/40 of the planetary circumference—that is, spherical harmonics up to degree and order 20 (on Earth, ~1000 km). On bodies shaped by processes like plate tectonics that generate relief at shorter wavelengths, we expect reduced correlation at long wavelengths, with gradual improvement as shorter-wavelength features that deflect rivers are included in the comparison. We further hypothesize that the timing of deformation and erosion influences global drainage patterns. If the establishment of a planet's topography is followed by a long period of tectonic quiescence, rivers will have more time to adjust to, and alter, that topography, and drainage directions will conform better with the long-wavelength component of the altered topography. On planets where tectonic deformation is more recent or more intense than fluvial erosion, shorter-wavelength topography related to this deformation will have a stronger influence on drainage directions, and long-wavelength conformity will be reduced.

To test these hypotheses, we compared global drainage patterns and long-wavelength topography for Earth, Mars, and Titan (Fig. 1). We focused on fluvially modified worlds, but we expect volcanic, cryovolcanic, and other fluid-flow features on bodies such as Venus and Pluto to leave similar signatures. We combined new and existing maps of drainages on Titan (*11*, *12*), Earth (*17*), and Mars (*18*) with spherical harmonic models for topography (*19*–*22*). We computed two proxy metrics for drainage conformity with topography (fig. S1). The first metric, the downhill percentage (%d), represents the proportion of points along a river that are at higher elevations than the next downstream point for a given point spacing and spherical harmonic expansion of topography (Fig. 2A). As topographic resolution becomes finer—in this case, as topography is expanded to higher spherical harmonic degrees—%d should approach 100% for active drainage networks because liquids in open channels flow downhill. The second metric, the conformity factor (Λ), is defined as Λ = median[cos(δ)], where δ is the angle between the river drainage direction and the downslope direction of the topographic expansion (Fig. 2B). Values of Λ closer to 1 indicate better agreement between flow directions and long-wavelength topography, but we do not expect perfect conformity (Λ = 1) at any resolution because we are comparing the steepest descent direction at a particular point to the flow direction across a finite interval.

Our results for topographic conformity as a function of maximum spherical harmonic degree are shown in Fig. 2. Conformity is consistently lower on Earth than on Mars or Titan, whereas Titan's conformity factor overlaps within uncertainty with that of Mars. The %d values are likewise much higher on Mars and Titan than on Earth. As expected, no body reaches near-perfect topographic conformity at the long wavelengths we consider here. These results lead us to the counterintuitive observation that many of Earth's

[1]Department of Earth and Atmospheric Science, City College of New York, City University of New York, New York, NY, USA. [2]Earth and Environmental Science, The Graduate Center, City University of New York, New York, NY, USA. [3]Department of Earth, Atmospheric, and Planetary Sciences, Massachusetts Institute of Technology, Cambridge, MA, USA. [4]Department of Earth and Planetary Science, University of California, Berkeley, Berkeley, CA, USA. [5]Division of Geological and Planetary Sciences, California Institute of Technology, Pasadena, CA, USA. [6]Department of Earth and Planetary Sciences, University of California, Santa Cruz, Santa Cruz, CA, USA. [7]Department of Geophysics, School of Earth Sciences, Stanford University, Stanford, CA, USA.
*Corresponding author. Email: bblack@ccny.cuny.edu

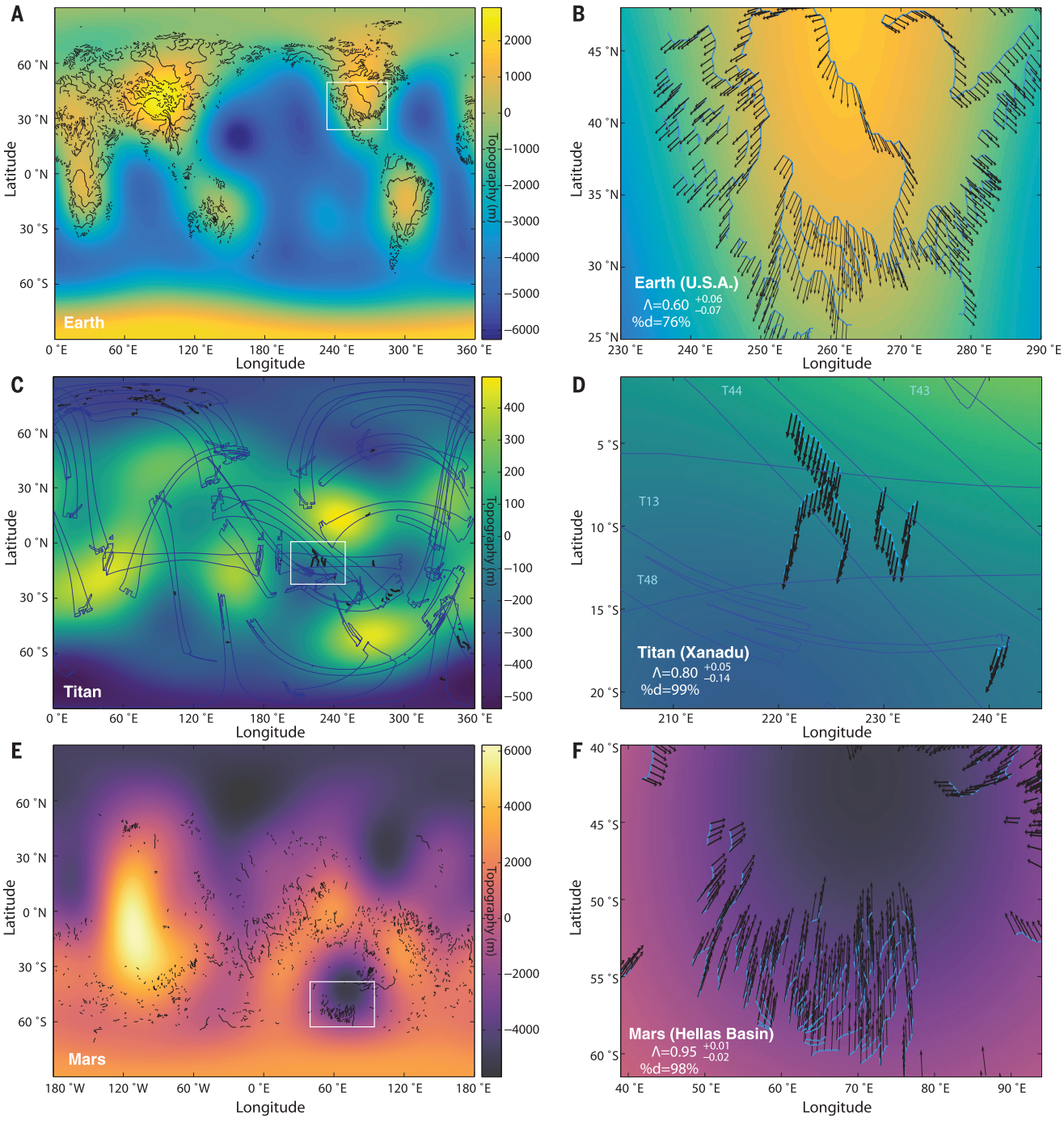

Fig. 1. Maps of topography referenced to the geoid and expanded to spherical harmonic degree and order 6, overlain with the fluvial features employed in this study. (**A**) Earth. (**B**) Enlargement of North America. (**C**) Titan. Blue outlines show Cassini Synthetic Aperture Radar (SAR) observation swaths. (**D**) Enlargement of eastern Shangri-La and Xanadu regions of Titan. T values represent the Cassini SAR swath numbers (swaths are outlined in blue). (**E**) Mars. (**F**) Enlargement of Hellas Basin on Mars. In (A), (C), and (E), white boxes outline regions enlarged in (B), (D), and (F), where river courses are shown in light blue, black arrows indicate topographic gradient at each point, and indicated conformity values span these enlarged regions, with uncertainties corresponding to the 95% confidence interval for the median (*19*).

rivers appear to flow along contour or uphill with respect to long-wavelength topography (as shown in Fig. 1B at locations where river traces deviate from gradient arrows), in contrast to most drainages on Titan and Mars.

On Mars, the strong correlation between valley network orientations and the present-day long-wavelength topography requires that most large-scale topography predates valley network formation in the Noachian era and that this ancient topography was the dominant influence on valley network orientation (Fig. 1F) (*1*, *2*, *23*). Martian topographic conformity remains imperfect even when shorter wavelengths are considered (fig. S5). We attribute this persistent, moderate disagreement between drainage directions and topography to the combined effects of impact cratering, topographic resolution, and deformation after the era of valley network formation (*24*, *25*). Because *%d* quantifies the proportion of river segments that flow from higher to lower topography (Fig. 2A

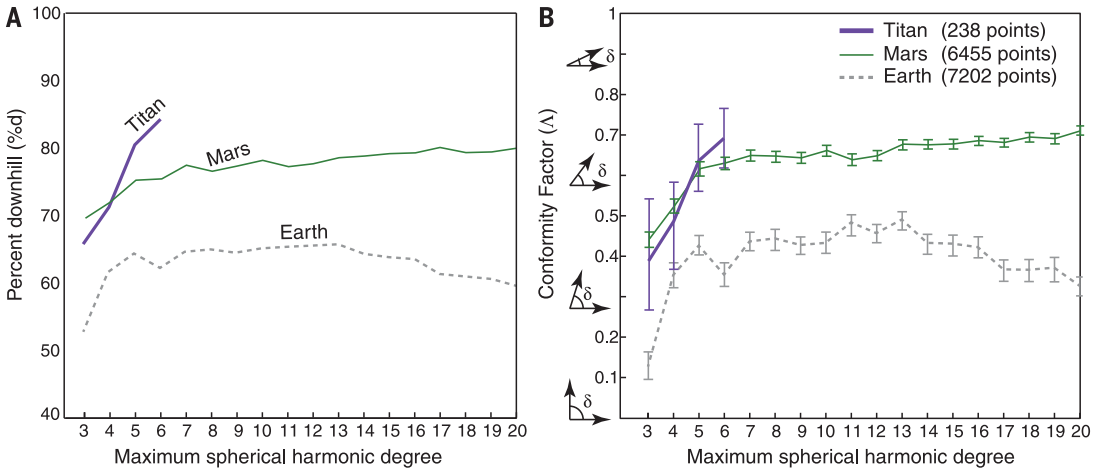

Fig. 2. Topographic conformity differs on Titan and Mars versus Earth. (**A**) The percent downhill (%*d*) metric as a function of the spatial resolution of the spherical harmonic expansion. (**B**) The conformity factor {Λ = median[cos(δ)]}. Angles corresponding to Λ values are illustrated on vertical axis. Uncertainties correspond to the 95% confidence interval for the median (*19*).

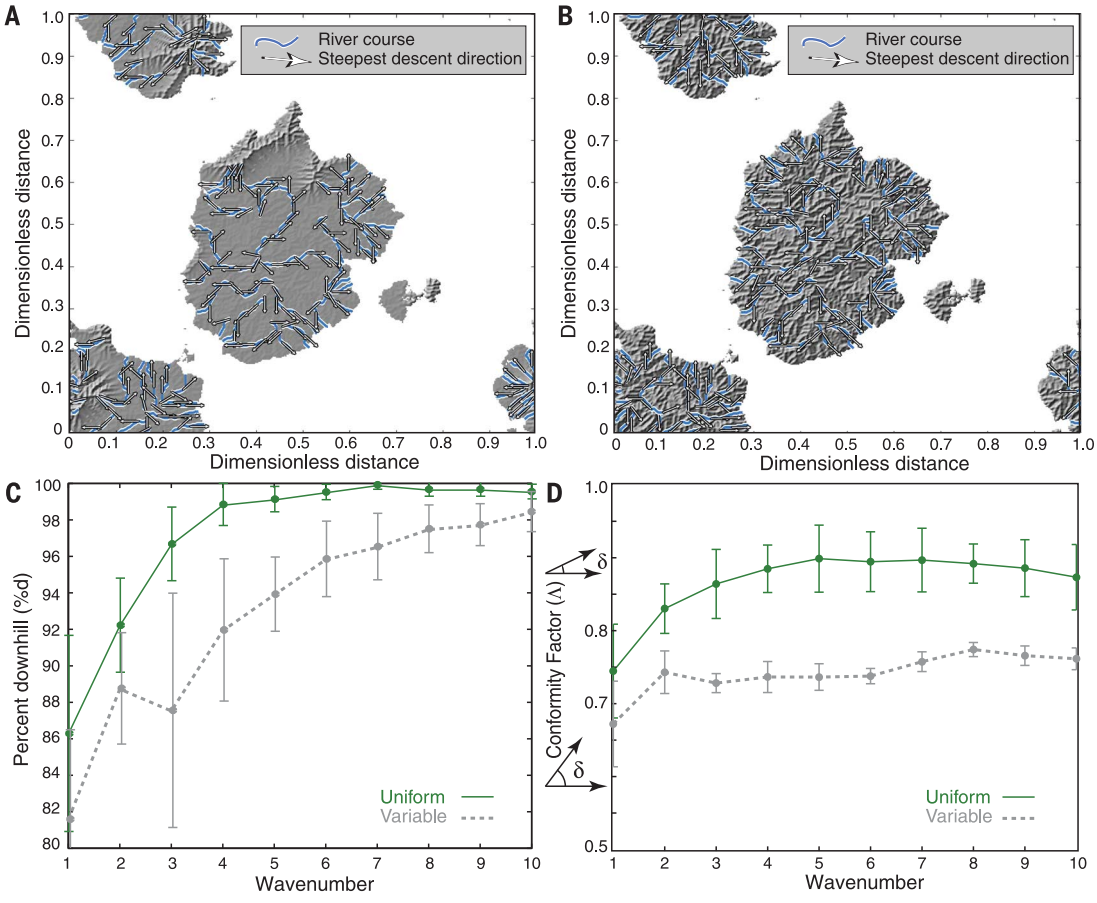

Fig. 3. Deformation history influences conformity. Variable-uplift simulations (**A**) represent plate tectonic–style–uplift, and uniform-uplift simulations (**B**) represent dominantly long-wavelength deformation. Shaded relief maps in (A) and (B) show simulations after 10 million years (My). The model domain is doubly periodic, and the lowest 70% of initial elevations (white) were set as the base level relative to which uplift occurs. (**C**) Mean %*d* among 10 variable-uplift simulations and 10 uniform-uplift simulations. (**D**) Mean topographic conformity among the same simulations analyzed in (C). In (C) and (D), error bars represent two standard errors of the mean across the simulation ensembles.

and fig. S5), our results place bounds on the amount of vertical deformation after the era of valley network formation. For at least 85% of the fluvially dissected landscapes on Mars, Hesperian and Amazonian era vertical deformation has not exceeded the initial relief.

For Titan, a similar analysis suggests that mid-latitude and equatorial topography has been stable since the formation of the fluvial networks. If present-day topography was shaped by an episode of nonuniform crustal thickening at 0.3 to 1.2 Ga (*16*, *26*), fluvial networks at middle and low latitudes must have formed after that time. In contrast, many of Titan's north polar networks deviate from regional gradients (fig. S3). This result is consistent with recent or ongoing predominantly short-wavelength deformation in the north polar region.

What processes have shaped the topographic conformity of Earth, Mars, and Titan? Multiple factors could plausibly contribute to weak long-wavelength topographic conformity, including little erosion relative to relief and resurfacing, low-amplitude long-wavelength topography, impact cratering, or vigorous short-wavelength deformation. However, Earth is deeply eroded, the topographic power spectra for the terrestrial planets are self-affine (i.e., the height of relief features scales with their wavelength), and topographic power spectra for Earth and Mars are almost identical (*20*, *27*). Consequently, neither weak erosion nor contrasts in global static topography can fully explain the low topographic conformity on Earth relative to Mars.

On Earth, plate tectonics preserves cratons—broad, flat regions where small changes in

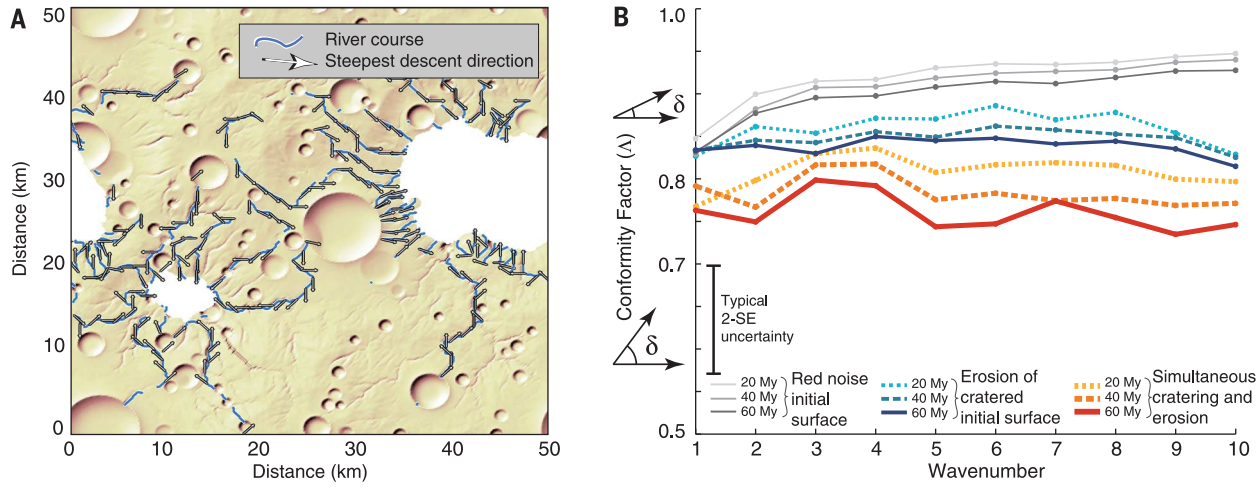

Fig. 4. Impact cratering can modulate topographic conformity. (**A**) Shaded relief map of a representative simulation after 60 My of erosion in tandem with impact cratering. (**B**) Mean topographic conformity among 10 control simulations, 10 simulations with a cratered initial surface, and 10 simulations with ongoing cratering in tandem with fluvial erosion. Times refer to model time after initiation (*19*). Legend shows a typical uncertainty of two standard errors of the mean within the simulation ensembles.

topography can yield large shifts in conformity—while driving short-wavelength, spatiotemporally variable rock uplift at active margins. To explore the influence of terrestrial plate tectonics on drainage network evolution, we analyzed river network conformity for a series of numerical landscape evolution model simulations (*19*, *28*). We completed two sets of ten idealized simulations: the first set with spatially uniform uplift to represent a world in which long-wavelength deformation dominates the production of relief (Fig. 3A) and the second set with spatially variable uplift to capture the effects of short-wavelength deformation on drainage orientations (Fig. 3B). The simulations with variable uplift are intended to investigate the particular influence of plate tectonics. According to both our metrics, drainage directions in the uniform-uplift simulations conform much better with long-wavelength topography than in the variable-uplift simulations (Fig. 3, C and D). The absolute magnitudes of Λ and %*d* are higher in the model than in natural drainage networks, partly because the model lacks cratons and sedimentary basins, both of which suppress conformity in nature. Nonetheless, our idealized model offers qualitative insights into the effects of variable uplift on drainage patterns. Active, spatially variable uplift depresses topographic conformity, but this effect is temporary: once the variable uplift ceases, the topographic conformity steadily increases (fig. S4A). Overall, the results support our hypothesis that short-wavelength active deformation (such as mountain-building on Earth) interferes with the background pattern of rivers draining the continents.

Geomorphic mapping shows that drainage basins on Mars are strongly influenced by preexisting ancient Noachian topography, including the hemispheric dichotomy, early Noachian impact structures, and subtle ridges of unknown origin located throughout the southern highlands (*2*, *23*). Cratering during and after the Late Heavy Bombardment ~4 Ga further disrupted some drainage basins (*2*, *23*, *24*). To quantify the extent of this disruption and the consequences for topographic conformity, we conducted additional landscape evolution simulations (*19*). We find that unless impacts obliterate drainages entirely, they can modify, but do not erase, alignment with preexisting long-wavelength topography (Fig. 4), consistent both with mapped relationships between drainage patterns and large-scale slopes (*1*, *2*, *23*) and with our measurements showing relatively high martian topographic conformity. Crustal magnetization (*29*) and >3.6-billion-year-old felsic rocks on Mars (*30*) have been interpreted as evidence for processes typically associated with plate tectonics on Earth. Our model results and the high conformity of Martian drainage networks suggest that at the time of martian river incision, plate tectonics was absent and impact cratering was insufficiently intense to fully disrupt drainage alignment with ancient long-wavelength topographic gradients (*1*, *2*, *5*, *23*).

Of the three bodies we consider here, Titan's geologic history is the most enigmatic. In contrast to the ancient long-wavelength topography of Mars (*1*, *4*), Titan shows evidence for recent or ongoing geologic activity (*11*, *16*, *26*). Titan's long-wavelength conformity thus implies that long-wavelength mechanisms actively dominate the generation of relief in most regions of Titan (the north polar region is a possible exception). A mechanism such as global-scale changes in shell thickness due to tidal heating or basal melting and refreezing would create both long-wavelength relief and local fractures on Titan (*7*, *31*). Titan's high topographic conformity supports geophysical arguments for substantial sediment transfer from topographic highs to lows (*31*). Patterns in Titan's atmospheric circulation are expected to result in net poleward transport of hydrocarbons from mid-latitudes (*32*). Of the drainages we mapped on Titan that are located poleward of 45°N and 45°S latitudes, and that traverse at least two degrees of latitude, five out of six drain toward the poles (Fig. 1 and database S1). This implies that other hydrocarbon fluxes or transport mechanisms must balance the net atmospheric and fluvial transport of hydrocarbons toward Titan's poles.

Topographic conformity does not reach the near-perfect %*d* predicted by the model on any of the three bodies we consider because of limited map resolution (*19*). Modest short-wavelength deformation, impact cratering, or deformation after the development of drainages (*5*, *25*) have probably also contributed to the imperfect conformity on Mars and Titan. The improvement of drainage alignment on Earth relative to Mars at very short wavelengths (*24*) supports this interpretation for Mars. In a set of landscape evolution simulations in which uplift ceases entirely after a period of variable uplift, we find that topographic gradients on the resulting low-relief surfaces (similar to Earth's cratons) can eventually grow weak and chaotic at shorter wavelengths, allowing drainage patterns to retain the imprint of past conditions (fig. S4B). On Earth, topographic conformity dips at scales of 750 to 1500 km, which we attribute to steep gradients in elevation from ocean basins to convergent margins to low-relief continental interiors.

Earth and Mars share similarly bimodal topography (*33*) but divergent global geology, proving that the distribution of elevations alone cannot reveal geologic evolution. The interaction of rivers with long-wavelength topography provides an alternative record of the generation of planetary relief. The formation and amalgamation of continental crust are processes that create dominantly long-wavelength topography, as is the process that built the martian hemispheric dichotomy. Construction of mountain ranges on Earth has a dominantly intermediate wavelength, necessarily smaller than the scale of continents. Martian drainage patterns reflect ancient long-wavelength

topography that predates both valley network formation and Noachian-Hesperian bombardment (*2*), confirming that Noachian Mars lacked global plate tectonics and bounding post-Noachian changes in martian relief. Our results favor dominantly long-wavelength relief-generating mechanisms on Titan such as shell-thickness variations arising from tidal heating (*6*, *7*) or thermal expansion and contraction (*6*). Together, the three river-worn bodies in our solar system provide a Rosetta stone for deciphering the imprint of tectonics on landscapes.

REFERENCES AND NOTES

1. R. J. Phillips *et al*., *Science* **291**, 2587–2591 (2001).
2. R. P. Irwin, A. D. Howard, *J. Geophys. Res. Planets* **107**, 10-1–10-23 (2002).
3. J. T. Perron, J. X. Mitrovica, M. Manga, I. Matsuyama, M. A. Richards, *Nature* **447**, 840–843 (2007).
4. J. C. Andrews-Hanna, M. T. Zuber, W. B. Banerdt, *Nature* **453**, 1212–1215 (2008).
5. S. Bouley *et al*., *Nature* **531**, 344–347 (2016).
6. G. C. Collins *et al*., in *Planetary Tectonics*, T. R. Watters, R. A. Schultz, Eds. (Cambridge Univ. Press, 2009), pp. 264–350.
7. F. Nimmo, B. Bills, *Icarus* **208**, 896–904 (2010).
8. J. M. Moore *et al*., *Science* **351**, 1284–1293 (2016).
9. S. D. Willett, S. W. McCoy, J. T. Perron, L. Goren, C. Y. Chen, *Science* **343**, 1248765 (2014).
10. A. D. Howard, J. M. Moore, R. P. Irwin, *J. Geophys. Res. Planets* **110**, E12S14 (2005).
11. B. A. Black, J. T. Perron, D. M. Burr, S. A. Drummond, *J. Geophys. Res. Planets* **117**, E08006 (2012).
12. D. M. Burr, S. A. Drummond, R. Cartwright, B. A. Black, J. T. Perron, *Icarus* **226**, 742–759 (2013).
13. C. Hoorn *et al*., *Science* **330**, 927–931 (2010).
14. H. V. Frey, J. H. Roark, K. M. Shockey, E. L. Frey, S. E. Sakimoto, *Geophys. Res. Lett.* **29**, 22-1–22-4 (2002).
15. C. I. Fassett, J. W. Head III, *Icarus* **195**, 61–89 (2008).
16. C. D. Neish, R. D. Lorenz, *Planet. Space Sci.* **60**, 26–33 (2012).
17. H. Wu *et al*., *Water Resour. Res.* **48**, W09701 (2012).
18. B. M. Hynek, M. Beach, M. R. Hoke, *J. Geophys. Res. Planets* **115**, E09008 (2010).
19. Materials and methods are available as supplementary materials.
20. M. A. Wieczorek, in *Treatise on Geophysics*, G. Schubert, Ed. (Elsevier, ed. 2, 2015), chap. 10.05, pp. 153–193.
21. H. A. Zebker *et al*., *Science* **324**, 921–923 (2009).
22. C. Hirt, M. Kuhn, W. Featherstone, F. Göttl, *J. Geophys. Res. Solid Earth* **117**, B05407 (2012).
23. R. P. Irwin III, R. A. Craddock, A. D. Howard, H. L. Flemming, *J. Geophys. Res. Planets* **116**, E02005 (2011).
24. W. Luo, T. Stepinski, *Geophys. Res. Lett.* **39**, L24201 (2012).
25. A. Lefort, D. M. Burr, F. Nimmo, R. E. Jacobsen, *Geomorphology* **240**, 121–136 (2014).
26. G. Tobie, J. I. Lunine, C. Sotin, *Nature* **440**, 61–64 (2006).
27. D. L. Turcotte, *J. Geophys. Res. Solid Earth* **92**, E597–E601 (1987).
28. J. T. Perron, W. E. Dietrich, J. W. Kirchner, *J. Geophys. Res. Earth Surf.* **113**, F04016 (2008).
29. F. Nimmo, D. Stevenson, *J. Geophys. Res. Planets* **105**, 11969–11979 (2000).
30. V. Sautter *et al*., *Nat. Geosci.* **8**, 605–609 (2015).
31. D. Hemingway, F. Nimmo, H. Zebker, L. Iess, *Nature* **500**, 550–552 (2013).
32. T. Schneider, S. D. B. Graves, E. L. Schaller, M. E. Brown, *Nature* **481**, 58–61 (2012).
33. R. D. Lorenz *et al*., *Icarus* **211**, 699–706 (2011).

ACKNOWLEDGMENTS

We thank E. Chan for spot-checking martian drainages. Three reviewers provided constructive feedback. B.A.B. acknowledges NASA grant NNX16AR87G. D.H. thanks the Miller Institute for Basic Research in Science. We thank the Cassini team. The topography and drainage data used in this paper are available at http://ddfe.curtin.edu.au/gravitymodels/Earth2012/ and http://eagle1.umd.edu/flood/DRT/ for Earth, at https://astrogeology.usgs.gov/search/map/Titan/Cassini/TitanFluvialMapping/TitanFluvialMapping_July2013 and in database S2 for Titan, and at https://webgis.wr.usgs.gov/pigwad/down/mars_dl.htm and http://pds-geosciences.wustl.edu/missions/mgs/megdr.html for Mars. The landscape evolution software Tadpole is available at https://github.com/MITGeomorph/Tadpole.

SUPPLEMENTARY MATERIALS

www.sciencemag.org/content/356/6339/727/suppl/DC1
Materials and Methods
Figs. S1 to S8
Tables S1 and S2
Databases S1 and S2
References (*34*–*55*)

1 June 2016; accepted 6 April 2017
10.1126/science.aag0171

Editor's Summary

River systems reveal planetary tectonics

Earth, Mars, and Titan have all hosted rivers at some point in their histories. Rivers erode the landscape, leaving behind signatures that depend on whether the surface topography was in place before, during, or after the period of liquid flow. Black *et al.* developed two metrics to measure how well river channels align with the surrounding large-scale topography (see the Perspective by Burr). Earth's plate tectonics introduce features such as mountain ranges that cause rivers to divert, processes that clearly differ from those found on Mars and Titan.

Science, this issue p. 727; see also p. 708